Pre-Fibrillation of Pulps to Manufacture Cellulose Nanofiber Reinforced High-Density Polyethylene using the Dry-Pulp Direct Kneading Method

Yuko Igarashi
Oji Holdings

Akihiro Sato
SEIKO PMC corporation

Hiroaki Okumura
Kyoto University: Kyoto Daigaku

Fumiaki Nakatsubo
Kyoto University: Kyoto Daigaku

Takashi Kuboki
Kyoto University: Kyoto Daigaku

Hiroyuki Yano (✉ yano@rish.kyoto-u.ac.jp)
Kyoto University: Kyoto Daigaku

Abstract

The dry-pulp direct-kneading method is an industrially viable, low-energy process to manufacture cellulose nanofiber (CNF) reinforced polymer composites, where chemically modified pulps can be nanofibrillated and dispersed uniformly in the polymer matrix during melt-compounding. In this study, cellulose fibers with different sizes, ranging from surface-fibrillated pulps with 20 μm in width to fine CNFs with 20 nm in width were prepared from softwood bleached kraft pulps (NBKPs) using a refiner and high-pressure homogenizer (HPH). These cellulose fibers were modified with alkenyl succinic anhydride (ASA), and then dried. The dried ASA-treated cellulose fibers were used as a feed material for melt-compounding in the dry-pulp direct kneading method to fabricate CNF reinforced high-density polyethylene (HDPE). When surface-fibrillated pulps were employed as a feed material, the pulps were nanofibrillated and dispersed uniformly in the HDPE matrix during the melt-compounding, and the composites had much better properties (i.e., much higher tensile modulus and strength and much lower coefficient of thermal expansion) than the composites produced using the pulps without pre-fibrillation. However, when CNFs were used as a feed material, the CNFs were shortened and agglomerated during the melt-compounding, thus deteriorating the properties of the composites. The study concludes that the pre-fibrillation of pulps had a significant impact on the morphology and properties of the composites. Unexpectedly, the surface-fibrillated pulp, which can be produced cost-effectively using a refiner at an industry scale, was a more suitable form than the CNF as a feed material for melt-compounding in the dry-pulp direct kneading method.

1. Introduction

A cellulose nanofiber (CNF) is a fundamental element of plant cell wall, where cellulose molecules are extended and form semi-crystalline structures(Moon et al. 2011). The extended and aligned cellulose molecules give a CNF excellent mechanical properties and coefficient of thermal expansion, which attracts industry to utilize CNFs to reinforce polymers. In fact, there is a great demand for CNF/polymer composites to be employed as automotive parts, electric appliance parts and building materials(Yano 2005; Moon et al. 2011; Abdul Khalil et al. 2012; Dufresne 2013; Miao and Hamad 2013; Oksman et al. 2016; Ramu et al. 2019). However, in spite of these attractive properties of a CNF, CNF/polymer composites have yet to expand in industrial application. One of the main reasons is a low affinity between hydrophilic CNFs and hydrophobic polymers. Due to hydrogen bonding between OH groups in CNFs, CNFs aggregate in hydrophobic polymers during melt-compounding. Therefore, many researchers have been trying to improve the low affinity by modifying CNF surface chemically (Hassan et al. 2014; Sato et al. 2016; Yano et al. 2018), adding compatibilizers (Qiu et al. 2005; Volk et al. 2015; Sakakibara et al. 2016; Suzuki et al. 2016), and/or modifying mixing process of CNFs and polymers (Hietala et al. 2013; Suzuki et al. 2013; Oksman et al. 2016).

Generally, CNF reinforced thermoplastic polymer composites are produced by firstly producing CNFs from pulps and then melt-compounding the CNFs and thermoplastic polymers (Wang and Sain 2007; Hietala et al. 2013; Abdul Khalil et al. 2014; Hassan et al. 2014). On the other hand, we have recently developed the

Dry-Pulp Direct-Kneading Method (Igarashi et al. 2018) to manufacture CNF reinforced thermoplastic polymer composites. In this method, pulps are modified with alkenyl succinic anhydride (ASA), and then dried. The dried, ASA-treated pulps are used as a feed material for melt-compounding with thermoplastic polymers, and the ASA-treated pulps are nanofibrillated and dispersed uniformly in the polymer matrix during the melt-compounding. This process enables to combine the two processes (i.e., the production of CNFs and melt-compounding of CNFs and thermoplastic polymers), thus reducing the manufacturing time, energy and cost significantly. Furthermore, this process increases the aspect ratio of fiber (length/width) by changing its width from micro-scale (pulp) to nano-scale (CNF) during the melt-compounding, and enhances mechanical properties of the composites. Therefore, if CNFs, rather than pulps, are used as a feed material for melt-compounding with thermoplastic polymers in the dry-pulp direct kneading method, the CNFs may be further fibrillated to finer CNFs, thus further improving mechanical properties of CNF reinforced thermoplastic polymer composites. However, effects of pre-fibrillation of pulps on morphology and mechanical property of the composites have not been reported before.

In this study, ASA-treated cellulose fibers with different sizes (from pulps with 20 μm in width to fine CNFs with 20 nm in width) were used as a feed material for melt-compounding with high-density polyethylene (HDPE) in the dry-pulp direct kneading method, and their effects on morphology, mechanical properties and coefficient of thermal expansion of the composites were investigated.

2. Materials And Methods

2.1. Materials

Softwood bleached kraft pulps (NBKPs) were supplied by Oji Holdings Corporation (Tokyo, Japan) as never-dried kraft pulps with a pulp content of 20–25wt% in water. The Canadian Standard Freeness (CSF), as per TAPPI standard T227om-09, of NBKPs were 720 mL. N-Methyl-2-pyrrolidone (NMP) was purchased from Mitsubishi Chemical Corporation (Tokyo, Japan). Alkenyl succinic anhydride (ASA) (T-NS135) was supplied by SEIKO PMC Corporation (Tokyo, Japan). Maleic anhydride-grafted polypropylene (MAPP) (TOYO-TAC, PMA-H1000P) was purchased from TOYOBO Co., Ltd (Osaka, Japan). The weight-average molecular weight and amount of maleic anhydride grafted were 7.2×10^4 g/mol and 5.74wt%, respectively, as stated by the supplier. HDPE powders (FLO-BEADS, HE3040, mp: 130°C) were purchased from SUMITOMO SEIKA Co., Ltd (Tokyo, Japan). The average particle size was 11 μm as stated by the supplier. HDPE pellets (J320, mp: 130°C) were purchased from Asahi Kasei Chemicals Co., Ltd (Tokyo, Japan). Calcium carbonate ($CaCO_3$) was purchased from Wako Pure Chemical Industries, Ltd. (Osaka, Japan). All the materials were used as received.

2.2. Pre-fibrillation of pulps

Cellulose fibers with different sizes, ranging from surface-fibrillated pulps to fine CNFs with 20 nm in width, were prepared from NBKPs using a refiner and high-pressure homogenizer (HPH). The NBKPs were

treated using a refiner until CSF was less than 100 mL. The degree of polymerization was 940, calculated from the value of relative viscosities, as per TAPPI standard T230om-99. The lignin content was 0wt% according to the Klason lignin method (TAPPI standard T230om-02). The refiner-treated pulps in water (0.5wt%, 2L) was disintegrated mechanically using a high-pressure homogenizer (HPH) (Star Burst 10, HJP-25008 K, Sugino Machine CO., Ltd., Japan) at 15°C. The nozzle size was 0.17 mm and pressure was ca. 200 MPa. The HPH treatments were repeated up to ten times.

In this study, 5 types of cellulose fibers were prepared: pulps without pre-fibrillation, pulps treated by the refiner and CNFs treated by the refiner and HPH (1 pass, 3 passes and 10 passes).

2.3. Field emission scanning electron microscopy

The cellulose fibers were observed using a field emission scanning electron microscope (FE-SEM, JSM-6700F; JEOL, Ltd., Tokyo, Japan) at an acceleration voltage of 1.5 kV. Before the observation, the cellulose fibers were coated with platinum using an ion sputter coater (Auto-Fine Coater JFC-1600; JEOL, Ltd., Tokyo, Japan).

2.4. X-ray diffraction

X-ray diffraction patterns of the cellulose fibers were obtained using an X-ray diffractometer (UltraX 18HF, Rigaku Corp., Tokyo, Japan) at 30 kV and 200 mA. The degrees of crystallization of the cellulose fibers were calculated with the method of Segal et al. (1959).

2.5. Dewatering time test of cellulose fiber suspension

A specially designed vacuum filter was used to characterize ease of removing water from suspensions of the cellulose fibers with different sizes. The filtration system was composed of a stainless-steel mesh sieve having a large aperture size and filter papers. Three sheets of quantitative ashless filter paper with a diameter of 185 mm (5A, Advantec Toyo Kaisha Ltd., Japan) were wetted with distilled water prior to the test. The filter papers were sandwiched between O-rings and put on the sieve. The filtration system was placed between two hollow cylinders. Six hundred grams of 0.1wt% cellulose fiber suspension was poured into the upper cylinder at 20°C. The suspension was then gently stirred before applying a vacuum of -30.3 kPa (± 0.4) to the lower cylinder. The filtration time of the cellulose fibers through the system was recorded.

2.6. Surface modification of cellulose fibers

All the cellulose fibers (i.e., the pulps without pre-fibrillation, pulps treated by the refiner and CNFs treated by the refiner and HPH) were modified with ASA in NMP. Since ASA reacts with water before reacting with OH groups of the cellulose fibers, water was replaced with an aprotic organic solvent, NMP, before the ASA treatment. Five hundred grams of wet cellulose fibers (solids content of 20−25wt%) and 450 g of NMP were mixed (Tri-mix TX-5; INOUE MFG., Inc. Kanagawa, Japan), followed by evaporation of water under reduced pressure at 20−60°C. ASA (80 g) in 50 g of NMP and 25 g of K_2CO_3 were added to the cellulose fiber/NMP, and the mixture was stirred for 1 hour at 70−80°C. The ASA-treated cellulose fibers

were washed with a series of acetone, ethanol, aqueous acetic acid, distilled water, and isopropanol to have ASA-treated cellulose fibers in isopropanol. Acetone and ethanol were used to gradually change polarity of the solvent into hydrophilic nature. Acetic acid was used to replace the ASA functional end structure COOK with COOH. Further information about the ASA treatment can be found elsewhere (Sato et al. 2016, 2019).

The degree of substitution (DS) of the cellulose fibers was calculated from the area of the 1740 cm^{-1} absorbance peak in Fourier transform infrared (FT-IR) spectrum. Attenuated total reflection infrared (ATR-IR) spectra were recorded using an FT-IR spectrometer (Spectrum One, Perkin Elmer) in the range of 600 to 4000 cm^{-1} at a resolution of 2 cm^{-1}. A spectrum was obtained by accumulating 16 scans and normalized using the 1315 cm^{-1} peak of the cellulose CH_2 vibration. The band of the C = O stretching vibration mode of the acyl group (from 1735 to 1750 cm^{-1}) increased significantly for the modified cellulose fibers, indicating that esterification occurred. The DS and the area of the 1740 cm^{-1} peak were correlated by titration of the cellulose fibers in advance. The DS of all the cellulose fibers prepared in this study was 0.4 ± 0.03.

2.7. Preparation of composites

Composites with the 5 types of the ASA-treated cellulose fibers were prepared. The ASA-treated cellulose fibers were mixed with MAPP, $CaCO_3$ and HDPE powders in isopropanol for 10 min using a propeller type mixer. The weight ratio of cellulose fiber:ASA:MAPP:$CaCO_3$:HDPE powders was 30:24:12.9:3:30. MAPP and $CaCO_3$ were added because the additions improved strength and strain at failure of the composites (Sato et al. 2016, 2019).

The isopropanol was filtered from the mixture under reduced pressure until the solid content reached about 50 wt%, and then the mixture was crushed in a mixer (waring blender). The crushed mixture was dried during mixing (Tri-mix TX-5; INOUE MFG., Inc. Kanagawa, Japan), and isopropanol was finally evaporated under reduced pressure at 20–60°C. The powders of the mixture and HDPE pellets were melt-compounded using a twin-screw extruder (KZW15-TW; Technovel Corp., Osaka, Japan) with a screw speed of 200 rpm and a feed rate of 50 g/h. The L/D (ratio of the screw length to diameter) and diameter of the extruder were 45 and 15 mm, respectively. The extruder includes six heating zones and the barrel temperatures were set from the zone next to the hopper at 110°C, 130°C, 130°C, 140°C, 140°C and 140°C, as shown in Fig. 1. The extrudate was cut into pellets using a pelletizer. The weight ratio of cellulose fiber:ASA:MAPP:$CaCO_3$:HDPE powders:HDPE pellets was 10:8:4.3:1:10:66.7 in the composite pellets.

Dumbbell-shaped specimens were prepared from the pellets using an injection molding machine (NPX7-1F; Nissei-Plastic Industrial Co., Ltd., Nagano, Japan) at an injection temperature of 160°C, an injection pressure of 100 MPa, an injection speed of 80 mm/s and a mold temperature of 40°C. The specimens had a length of 60 mm, a width of 5 mm at the neck and a thickness of 1 mm. Figure 2 summarizes the procedure for fabricating the composites described above.

2.8. Tensile test

Tensile properties of the composites were measured using a universal testing machine (Model 3655; Instron Corp., Canton, MA, USA) with a crosshead speed of 10 mm/min at 23°C. The load cell of the machine was 5 kN. Strain at failure was measured using a video camera. Tensile modulus was calculated from the stress-strain curve. Five specimens were tested and the average values were reported.

2.9. Thermomechanical test

Coefficient of thermal expansion (CTE) of the composites was acquired using a thermomechanical analyzer (TMA/SS6100, SII Nanotechnology Inc., Japan). A specimen was 30 mm long, 1 mm thick and 5 mm wide. Before measurement, the specimen was heated at 110°C for 48 h to remove moisture and then allowed to cool in a desiccator. The original grip distance was 20 mm and the specimen was tested under a tensile load of 29.4 mN. Measurement was performed in the range of -5° to 130°C at a heating rate of 5°C/min under a nitrogen atmosphere (60 ml/min). CTE was evaluated as the fractional change in length per degree of temperature change in the range of 0°C to 60°C.

2.10. X-ray computed tomography

Dispersibility and degree of fibrillation of cellulose fibers in the composites was observed using a X-ray computed tomography (CT) (SKY Scan 1172 instrument, Bruker-Micro CT, Kontich, Belgium). Observations were performed at the center of the dumbbell-shaped specimen.

2.11. Extraction of cellulose fibers from composites

To remove the HDPE matrix from composites, the composite sample was placed in a stainless-steel mesh container, and the container was immersed and stirred in boiling p-xylene (160°C). The sheet-like cellulose fibers left in the stainless-steel mesh were used to observe degree of fibrillation of cellulose fibers in the composites using the FE-SEM. In addition, to measure length of cellulose fibers in the composites, the cellulose fibers left in the stainless-streel mesh were dispersed into ethanol (0.001 wt%). The dilute solution was placed and dried on a glass plate for FE-SEM observation. Lengths of 100 cellulose fibers were measured from the FE-SEM images.

3. Results And Discussion

3.1 Pre-fibrillation of pulps

Figure 3 and Fig. 4 show, respectively, optical micrographs and FE-SEM micrographs of the cellulose fibers treated using the refiner and HPH. It is noted that in the FE-SEM micrographs (Fig. 4), the scale bars for the pulps without pre-fibrillation and refiner-treated pulps are 100 μm while those for the HPH-treated pulps are 1 μm. Both figures indicated that the degree of fibrillation increased through the refiner and subsequent HPH treatments. Most of the refiner-treated pulps were not fibrillated to CNFs but their surfaces were fibrillated, which suggests that external fibrillation of the pulps occurred. The external fibrillation is cutting or removal of the primary wall and the outer layer of the secondary wall (S_1 layer) of

a pulp, which allows fluffing the pulp surface and accelerates fibrillation of the inner walls (S_2 and S_3 layers) of a pulp (Uetani and Yano 2011).

A high-pressure homogenizer (HPH) is often used to manufacture CNFs from pulps (Baati et al. 2018; Phanthong et al. 2018). Unlike a bead mill, HPH does not cause contamination during the fibrillation process. In this study, HPH was used to fibrillate the refiner-treated pulps. After the refiner-treated pulps passed through the HPH (1 passage of the fibers through the HPH), fibers with a wide range of width were produced. Some surface fibrillated pulps were fibrillated to CNFs with 20–100 nm in width, suggesting that internal fibrillation (i.e., delamination and fibrillation of the inner S_2 and S_3 layers) occurred, while some surface-fibrillated pulps with about 20 μm in width were remained. After 3 passages of the fibers through the HPH, most of the fibers were CNFs with 20–100 nm in width, but some micro-sized fibers with several μm in width (named CMFs hereafter) were observed. After 10 passages of the fibers through the HPH, the fibers became fine CNFs with around 20 nm in width and either pulps or CMFs were not observed.

It is known that fibrillation of pulps under high shear stress can decrease crystallinity of cellulose fibers, which may affect reinforcing efficiency of cellulose fibers (Iwamoto et al. 2007; Ho et al. 2015). X-ray diffraction patterns and crystallinities of the refiner-treated pulps and HPH-treated (1 pass, 3 passes and 10 passes) CNFs are shown in Fig. 5 and Table 1, respectively. All the cellulose fibers had similar diffraction patterns and crystallinities, which indicates that the HPH treatments had little effect on the crystal structure and crystallinity of the cellulose fibers prepared in this study.

It is not an easy task to quantify the degree of fibrillation of cellulose fibers with a wide range of sizes (from pulps to fine CNFs) using a single experimental method. The Canadian Standard Freeness (CSF) test was conducted for the pulps and CNFs produced in this study. However, the HPH-treated CNFs were too small to measure their freeness. Therefore, viscosities of water solution of the cellulose fibers as well as the specific surface area of the cellulose fibers were measured. These two test methods reflected difference in the degree of fibrillation between the CNFs and fine CNFs but could not detect the difference between the pulps without pre-fibrillation and surface-fibrillated pulps. Consequently, the dewatering time test was used to characterize the degree of fibrillation of the cellulose fibers used in this study. The dewatering time test successfully measured the time required for filtration of cellulose fiber-water slurry for all the cellulose fibers, ranging from the pulps without pre-fibrillation to the fine CNFs. As listed in Table 1, the dewatering time increased with increasing the degree of fibrillation. In particular, the dewatering time of the HPH-treated (1 pass) CNFs was about 8 times longer than that of the refiner-treated pulps, which mirrors the significant difference in the degree of fibrillation between the HPH-treated (1 pass) CNFs and the refiner-treated pulps (see Figs. 3 and 4). It should also be noted that such a longer dewatering time causes a large increase in the cost to produce dried HPH-treated (1 pass) CNFs, which is not favorable to industrial setting.

Table 1
Dewatering time of cellulose fiber-water slurry and crystallinity of cellulose fibers.

Cellulose fiber	Dewatering time (s)	Crystallinity (%)
Pulps without pre-fibrillation	6	75.1
Refiner-treated pulps	40	76.2
HPH-treated (1 pass) CNFs	318	76.9
HPH-treated (3 passes) CNFs	636	74.7
HPH-treated (10 passes) CNFs	1644	78.4

3.2 Mechanical properties and CTE of composites

Typical stress–strain curves of the composites from tensile tests are shown in Fig. 6, and the mechanical properties (tensile modulus, tensile strength, and strain at failure) are summarized in Table 2. Meanwhile, elongation-temperature curves of the composites from thermomechanical tests are shown in Fig. 7, and the CTE values are summarized in Table 2. Since the HPH treatments facilitated nanofibrillation of the refiner-treated pulps, it may be expected that the HPH-treated CNFs have higher reinforcing efficiency than the refiner-treated pulps. However, the composites produced using the refiner-treated pulps and the HPH-treated (1 pass) CNFs had similar tensile modulus, tensile strength and CTE, as shown in Table 2. Interestingly, further increase of the number of passages through the HPH caused deterioration of the properties (i.e., decrease in tensile modulus and strength and increase in CTE). It should be noted that the properties of the composites produced using the HPH-treated (10 passes) CNFs are similar to those of the composites produced using the pulps without pre-fibrillation.

Table 2
Summary of mechanical properties and CTE of composites. The standard deviations are indicated in parentheses.

Sample	Tensile modulus (GPa)	Tensile strength (MPa)	Strain at failure (%)	CTE (10^6/K)
HDPE	1.08 (0.01)	23 (0.15)	>100	205
Composites using pulps without pre-fibrillation	2.46 (0.08)	43 (0.69)	4.1 (0.10)	88
Composites using refiner-treated pulps	3.46 (0.11)	56 (0.79)	3.2 (0.07)	54
Composites using HPH-treated (1 pass) CNFs	3.49 (0.07)	55 (0.92)	3.3 (0.05)	65
Composites using HPH-treated (3 passes) CNFs	3.21 (0.04)	53 (0.48)	3.4 (0.07)	69
Composites using HPH-treated (10 passes) CNFs	2.48 (0.07)	47 (0.43)	4.4 (0.21)	92

3.3 Morphology of composites

Cellulose fibers in the HDPE matrix were observed using X-ray CT (Fig. 8) and FE-SEM (Fig. 9). The X-ray CT image shows density distribution in three-dimensional space with special resolution of 700 nm. In Fig. 8, the HDPE matrix, which has a lower density than cellulose fibers, is shown in blue and cellulose fibers larger than 700 nm are shown in white. It is noted that the cellulose fibers observed in the X-ray CT images were pulps and CMFs while CNFs could not be detected because their width was beyond the spatial resolution of the X-ray CT. Both figures indicated that the composites produced using the pulps without pre-fibrillation had many large fibers with about 10 μm in width, which suggests that nanofibrillation of the pulps without pre-fibrillation did not occur during the melt-compounding. However, the composites produced using the refiner-treated pulps had many CNFs with 20–100 nm in width and some CMFs with several μm in width, and these fibers were dispersed uniformly in the HDPE matrix. The result suggests that the surface-fibrillation of pulps using the refiner promoted nanofibrillation of the pulps as well as uniform dispersion of the CNFs during the melt-compounding.

When the HPH-treated (1 pass and 3 passes) CNFs were used as a feed material, the composites had many CNFs with 20–100 nm in width and some CMFs with several μm in width. Their morphologies were similar to that of the composites produced using the refiner-treated pulps. In contrast, the composites

produced using the HPH-treated (10 passes) CNFs had agglomeration of CNFs (see the increase of spherical white regions in the X-ray CT image (Fig. 9)).

Figure 10 shows length frequency distribution of the cellulose fibers. The composites produced using the refiner-treated pulps and the HPH-treated (1 pass) CNFs had longer fibers than those produced using the HPH-treated (3 passes and 10 passes) CNFs. It is noted that the composites produced using the pulps without pre-fibrillation had long fibers (i.e., lengths of all the measured fibers were greater than 0.15 mm) though the results are not shown in the figure.

Table 3 summarizes relationships between the pre-fibrillation of pulps, morphology of the composites and properties of the composites. The surface-fibrillated pulps were nanofibrillated during the melt-compounding while maintaining a high aspect ratio (i.e., length/width) and uniform dispersion of CNFs in the HDPE matrix, thus giving good performance. The results suggested that the surface-fibrillated pulp was a suitable form as a feed material for the melt-compounding, and CNF is not a necessary form as a feed material for the melt-compounding. This enables to remove a preliminary step to prepare CNFs from pulps using a time consuming and energy intensive process, such as HPH, grinder and bead mill (Ho et al. 2015). Furthermore, the excessive use (i.e., multiple passes) of the HPH deteriorated the properties of the composites due to the agglomeration of fine CNFs during the melt-compounding. The excessive use of the HPH also reduced length of CNFs. It is speculated that the shorter CNFs moved more easily to agglomerate during the melt-compounding.

The finding of the agglomeration of the fine CNFs indicates that when fine CNFs are used as a feed material, properties of the composites can be improved by mitigating the agglomeration. Melt-compounding is capable of dispersing and distributing CNFs in the polymer matrix by mixing CNFs and molten polymer. However, when CNFs, including chemically modified CNFs, have low affinity for the polymer matrix such as HDPE, the mixing action would facilitate separation of the CNFs from the polymer matrix (i.e., agglomeration of the CNFs) rather than dispersion and distribution of the CNFs in the polymer matrix. Furthermore, when fine CNFs such as the HPH-treated (3 passes and 10 passes) CNFs are mixed with molten polymer, the mixing action would promote breakage of the fine CNFs, which would encourage agglomeration of the fine CNFs. Consequently, when fine CNFs are used as a feed material, agglomeration of the fine CNFs during melt-compounding may be prevented (1) by further improving the affinity between the fine CNF and HDPE and/or (2) by avoiding breakage of the fine CNFs during the melt-compounding. Further research is needed to solve the problem of the agglomeration of the fine CNFs.

Table 3
Summary of pre-fibrillation of pulps, morphology of composites and properties of composites.

Process for pre-fibrillation	Form of ASA-treated cellulose fiber before melt-compounding	Form of ASA-treated cellulose fiber after melt-compounding	Length and dispersion of fibers in composites	Ranking of properties of composites*
None	Pulp	Pulp	- Long fibers - Uniform dispersion	5
Refiner	Surface-fibrillated pulp	CNF (major) and CMF (minor)	- Long fibers - Uniform dispersion	1
Refiner and HPH (1 pass)	Surface-fibrillated pulp and CNF	CNF (major) and CMF (minor)	- Long fibers - Uniform dispersion	1
Refiner and HPH (3 passes)	CNF (major) and CMF (minor)	CNF (major) and CMF (minor)	- Short fibers - Uniform dispersion	3
Refiner and HPH (10 passes)	Fine CNF	Fine CNF	- Short fibers - Agglomeration	4

* The properties include tensile modulus, tensile strength and CTE.

4. Conclusion

The dried, ASA-treated cellulose fibers with different sizes, ranging from pulps with 20 μm in width to fine CNFs with 20 nm in width, were used as a feed material for melt-compounding in the dry-pulp direct kneading method to fabricate CNF reinforced HDPE. When the pulps without pre-fibrillation were fed into the twin-screw extruder, the pulps were not nanofibrillated during the melt-compounding, and the resulting composites had low tensile modulus and strength and high coefficient of thermal expansion. On the other hand, when the pulps were pre-fibrillated using the refiner, only surface of the pulps was fibrillated without sacrificing their internal structure. The surface-fibrillated pulps were nanofibrillated during the melt-compounding and the CNFs were dispersed uniformly in the HDPE matrix. The composites had much better properties (i.e., much higher tensile modulus and strength, as well as much lower coefficient of thermal expansion) than the composites produced using the pulps without pre-fibrillation. The 1-pass HPH treatment of the refiner-treated pulps changed the surface-fibrillated pulps into CNFs. Nevertheless, when the HPH-treated (1 pass) CNFs were used as a feed material for the melt-compounding, the composites had similar morphology and properties to the composites produced using the surface-fibrillated pulps (i.e., refiner-treated pulps). The further HPH treatments (i.e., increase in the number of

passages of CNFs through the HPH) had the CNFs finer. However, the finer CNFs were shortened and agglomerated during the melt-compounding and thus deteriorated the properties of the composites. The study concludes that the pre-fibrillation process of the pulps significantly affected the morphology and properties of the composites. The form of the cellulose fiber suitable for melt-compounding in the dry-pulp direct kneading method was the surface-fibrillated pulp, which can be produced cost-effectively using a refiner at an industry scale, rather than the CNF. The study also indicates that when fine CNFs are used as a feed material, properties of the composites can be improved by mitigating agglomeration of the fine CNFs, and suggests that agglomeration of the fine CNFs during melt-compounding may be prevented (1) by further improving the affinity between the fine CNF and HDPE and/or (2) by avoiding breakage of the fine CNFs during the melt-compounding.

Declarations

References

1. Abdul Khalil HPS, Bhat AH, Ireana Yusra AF (2012) Green composites from sustainable cellulose nanofibrils: A review. Carbohydr Polym 87:963–979. https://doi.org/10.1016/j.carbpol.2011.08.078

2. Abdul Khalil HPS, Davoudpour Y, Islam MN, et al (2014) Production and modification of nanofibrillated cellulose using various mechanical processes: A review. Carbohydr Polym 99:649–665. https://doi.org/10.1016/j.carbpol.2013.08.069

3. Baati R, Mabrouk A Ben, Magnin A, Boufi S (2018) CNFs from twin screw extrusion and high pressure homogenization: A comparative study. Carbohydr Polym 195:321–328. https://doi.org/10.1016/j.carbpol.2018.04.104

4. Dufresne A (2013) Nanocellulose: A new ageless bionanomaterial. Mater Today 16:220–227. https://doi.org/10.1016/j.mattod.2013.06.004

5. Hassan ML, Mathew AP, Hassan EA, et al (2014) Improving cellulose/polypropylene nanocomposites properties with chemical modified bagasse nanofibers and maleated polypropylene. J Reinf Plast Compos 33:26–36. https://doi.org/10.1177/0731684413509292

6. Hietala M, Mathew AP, Oksman K (2013) Bionanocomposites of thermoplastic starch and cellulose nanofibers manufactured using twin-screw extrusion. Eur Polym J 49:950–956. https://doi.org/10.1016/j.eurpolymj.2012.10.016

7. Ho TTT, Abe K, Zimmermann T, Yano H (2015) Nanofibrillation of pulp fibers by twin-screw extrusion. Cellulose 22:421–433. https://doi.org/10.1007/s10570-014-0518-6

8. Igarashi Y, Sato A, Okumura H, et al (2018) Manufacturing process centered on dry-pulp direct kneading method opens a door for commercialization of cellulose nanofiber reinforced composites. Chem Eng J 354:563–568. https://doi.org/10.1016/j.cej.2018.08.020

9. Iwamoto S, Nakagaito AN, Yano H (2007) Nano-fibrillation of pulp fibers for the processing of transparent nanocomposites. Appl Phys A Mater Sci Process. https://doi.org/10.1007/s00339-007-4175-6

10. Miao C, Hamad WY (2013) Cellulose reinforced polymer composites and nanocomposites: A critical review. Cellulose 20:2221–2262. https://doi.org/10.1007/s10570-013-0007-3

11. Moon RJ, Martini A, Nairn J, et al (2011) Cellulose nanomaterials review: Structure, properties and nanocomposites

12. Oksman K, Aitomäki Y, Mathew AP, et al (2016) Review of the recent developments in cellulose nanocomposite processing. Compos Part A Appl Sci Manuf 83:2–18. https://doi.org/10.1016/j.compositesa.2015.10.041

13. Phanthong P, Reubroycharoen P, Hao X, et al (2018) Nanocellulose: Extraction and application. Carbon Resour Convers 1:32–43. https://doi.org/10.1016/j.crcon.2018.05.004

14. Qiu W, Zhang F, Endo T, Hirotsu T (2005) Isocyanate as a compatibilizing agent on the properties of highly crystalline cellulose/polypropylene composites. J Mater Sci 40:3607–3614. https://doi.org/10.1007/s10853-005-0790-9

15. Ramu P, Jaya Kumar C V., Palanikumar K (2019) Mechanical characteristics and terminological behavior study on natural fiber nano reinforced polymer composite - A review. Mater Today Proc 16:1287–1296. https://doi.org/10.1016/j.matpr.2019.05.226

16. Sakakibara K, Yano H, Tsujii Y (2016) Surface Engineering of Cellulose Nanofiber by Adsorption of Diblock Copolymer Dispersant for Green Nanocomposite Materials. ACS Appl Mater Interfaces 8:24893–24900. https://doi.org/10.1021/acsami.6b07769

17. Sato A, Kabusaki D, Okumura H, et al (2016) Surface modification of cellulose nanofibers with alkenyl succinic anhydride for high-density polyethylene reinforcement. Compos Part A Appl Sci Manuf 83:72–79. https://doi.org/10.1016/j.compositesa.2015.11.009

18. Sato A, Yoshimura T, Kabusaki D, et al (2019) Multi-functional effect of alkenyl-succinic-anhydride-modified microfibrillated celluloses as reinforcement and a dispersant of CaCO3 in high-density polyethylene. Cellulose. https://doi.org/10.1007/s10570-019-02544-4

19. Segal L, Creely JJ, Martin AE, Conrad CM (1959) An Empirical Method for Estimating the Degree of Crystallinity of Native Cellulose Using the X-Ray Diffractometer. Text Res J. https://doi.org/10.1177/004051755902901003

20. Suzuki K, Homma Y, Igarashi Y, et al (2016) Investigation of the mechanism and effectiveness of cationic polymer as a compatibilizer in microfibrillated cellulose-reinforced polyolefins. Cellulose 23:623–635. https://doi.org/10.1007/s10570-015-0845-2

21. Suzuki K, Okumura H, Kitagawa K, et al (2013) Development of continuous process enabling nanofibrillation of pulp and melt compounding. Cellulose 20:201–210.

https://doi.org/10.1007/s10570-012-9843-9

22. Uetani K, Yano H (2011) Nanofibrillation of wood pulp using a high-speed blender. Biomacromolecules 12:348–353. https://doi.org/10.1021/bm101103p

23. Volk N, He R, Magniez K (2015) Enhanced homogeneity and interfacial compatibility in melt-extruded cellulose nano-fibers reinforced polyethylene via surface adsorption of poly(ethylene glycol)-block-poly(ethylene) amphiphiles. Eur Polym J 72:270–281. https://doi.org/10.1016/j.eurpolymj.2015.09.025

24. Wang B, Sain M (2007) Isolation of nanofibers from soybean source and their reinforcing capability on synthetic polymers. Compos Sci Technol 67:2521–2527. https://doi.org/10.1016/j.compscitech.2006.12.015

25. Yano H (2005) Optically transparent composites reinforced with networks of bacterial nanofibers. Sustain Humanosph 11. https://doi.org/10.1002/adma.200400597

26. Yano H, Omura H, Honma Y, et al (2018) Designing cellulose nanofiber surface for high density polyethylene reinforcement. Cellulose 25:3351–3362. https://doi.org/10.1007/s10570-018-1787-2
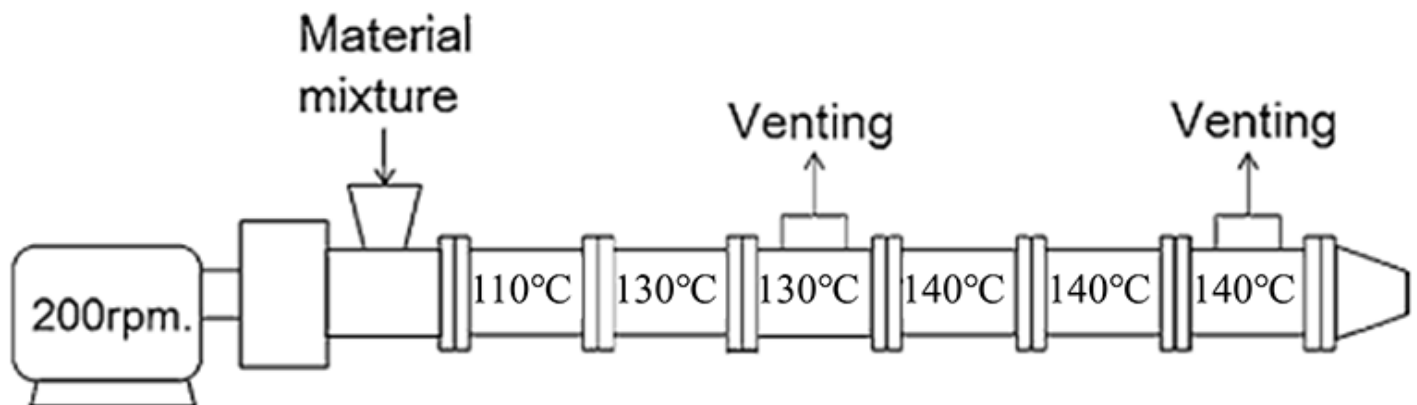
Figures

Figure 1

Barrel temperatures set in the twin-screw extruder.
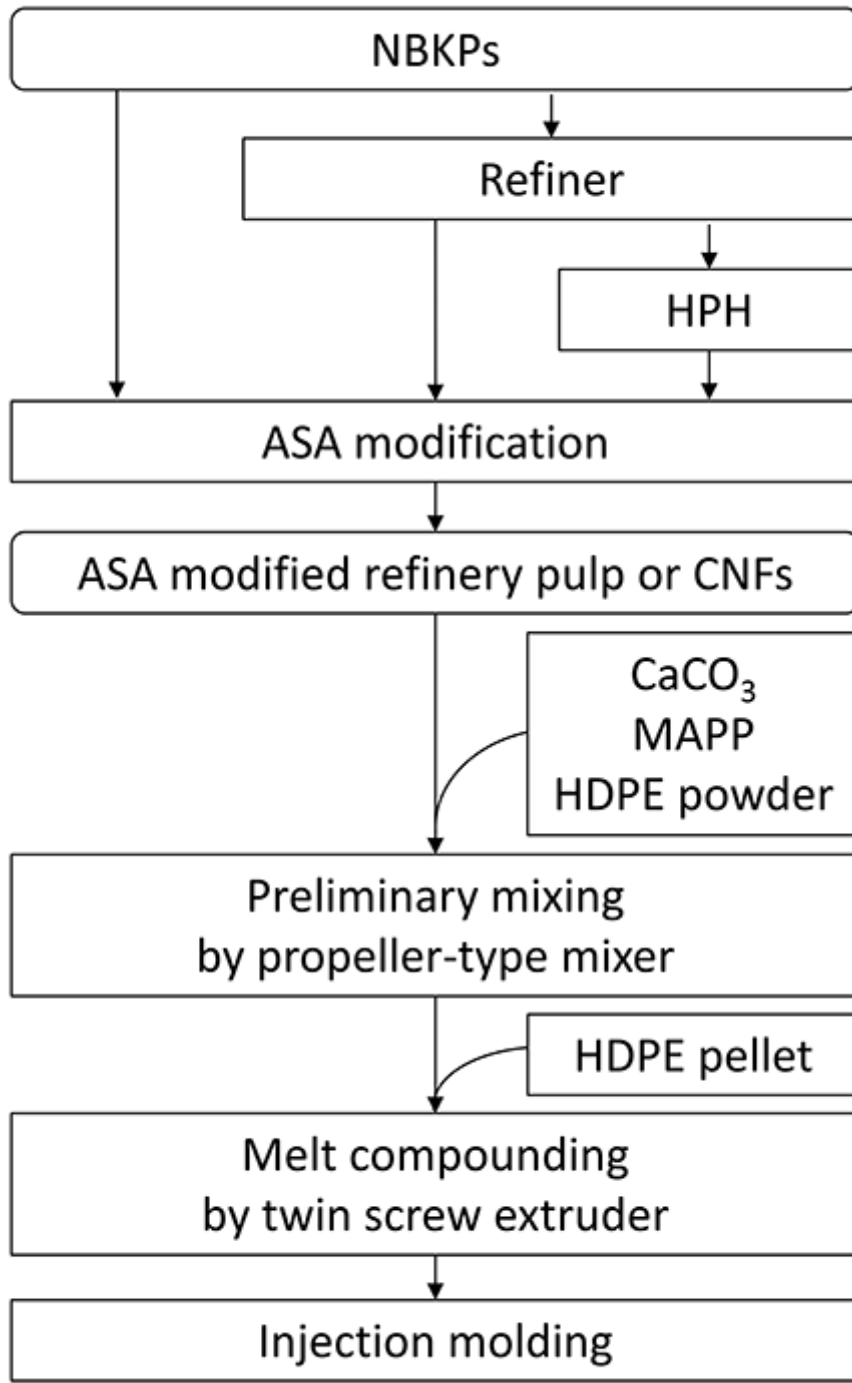
Figure 2

Procedure for fabricating composites.
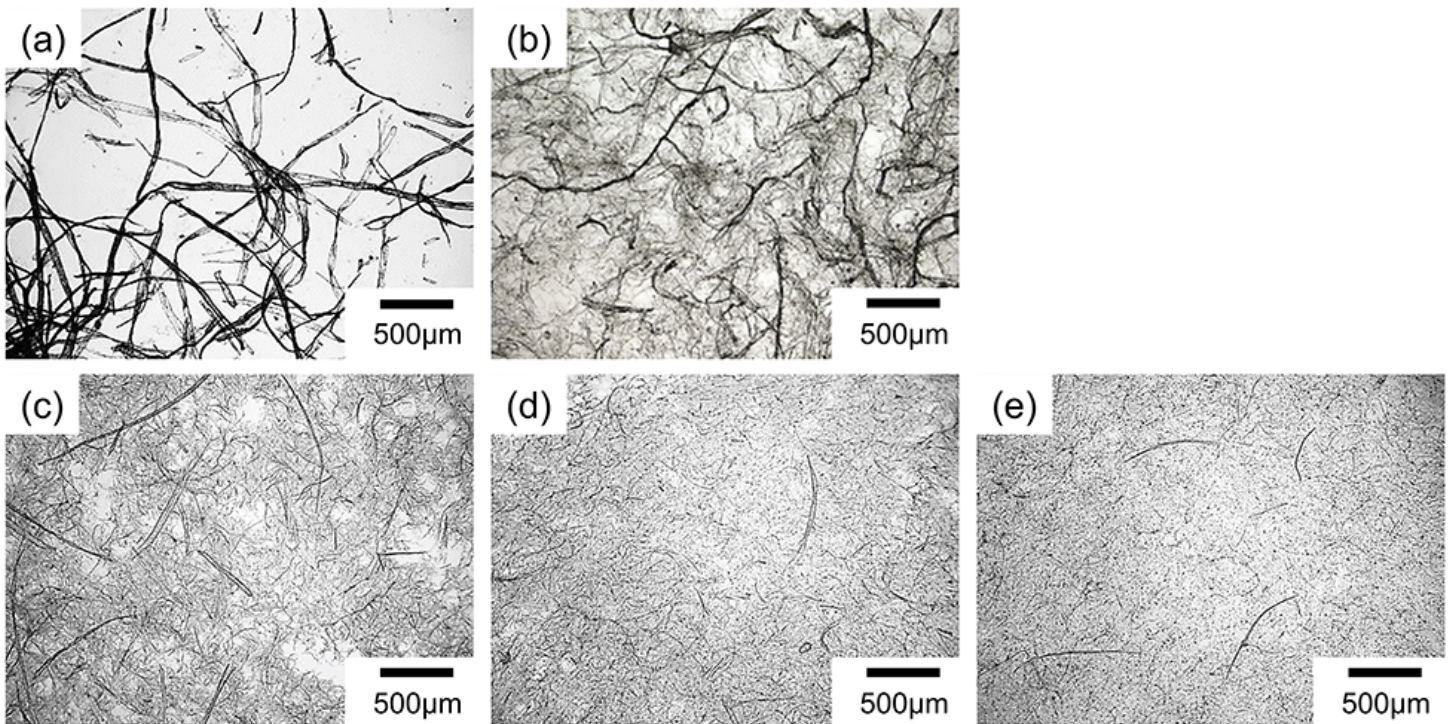
Figure 3

Optical micrographs of cellulose fibers: (a) pulps without pre-fibrillation, (b) refiner-treated pulps, (c) HPH-treated (1 pass) CNFs, (d) HPH-treated (3 passes) CNFs and (e) HPH-treated (10 passes) CNFs.
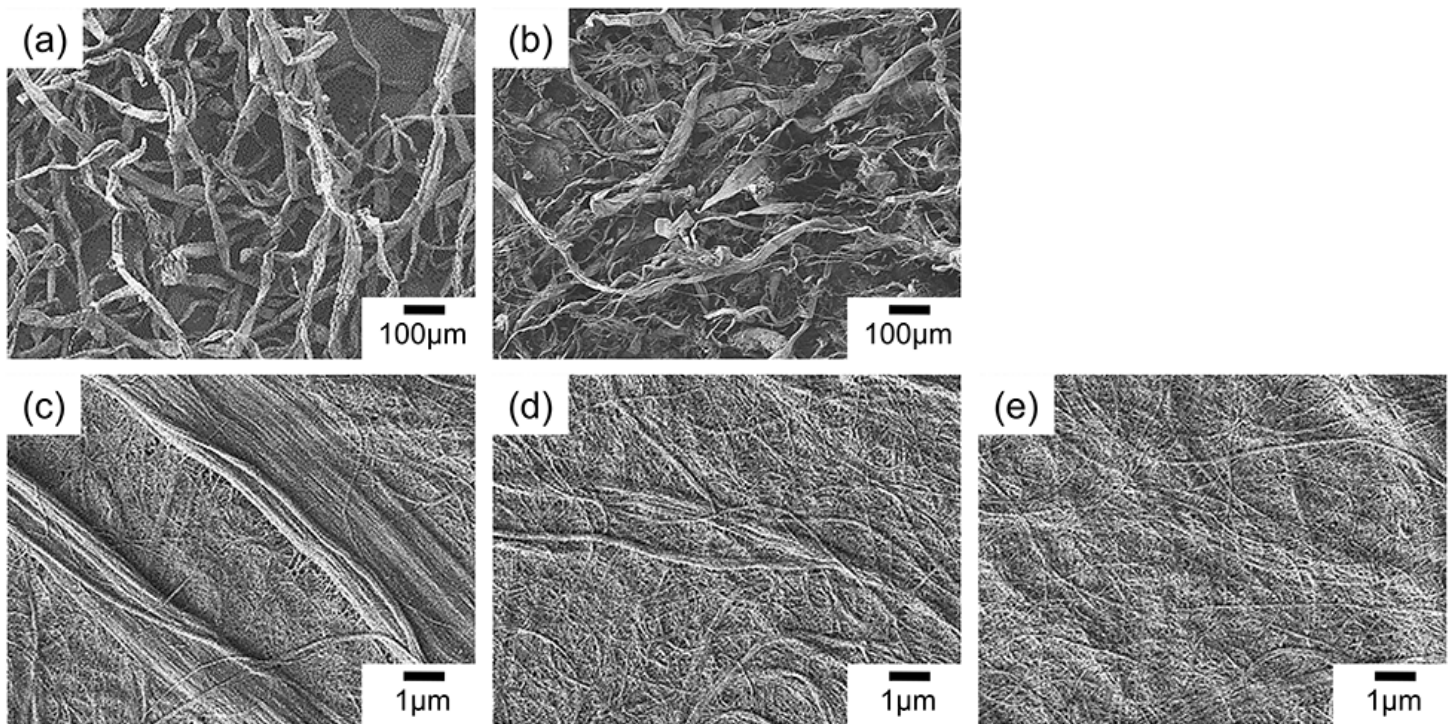

Figure 4

FE-SEM images of cellulose fibers: (a) pulps without pre-fibrillation, (b) refiner-treated pulps, (c) HPH-treated (1 pass) CNFs, (d) HPH-treated (3 passes) CNFs and (e) HPH-treated (10 passes) CNFs.
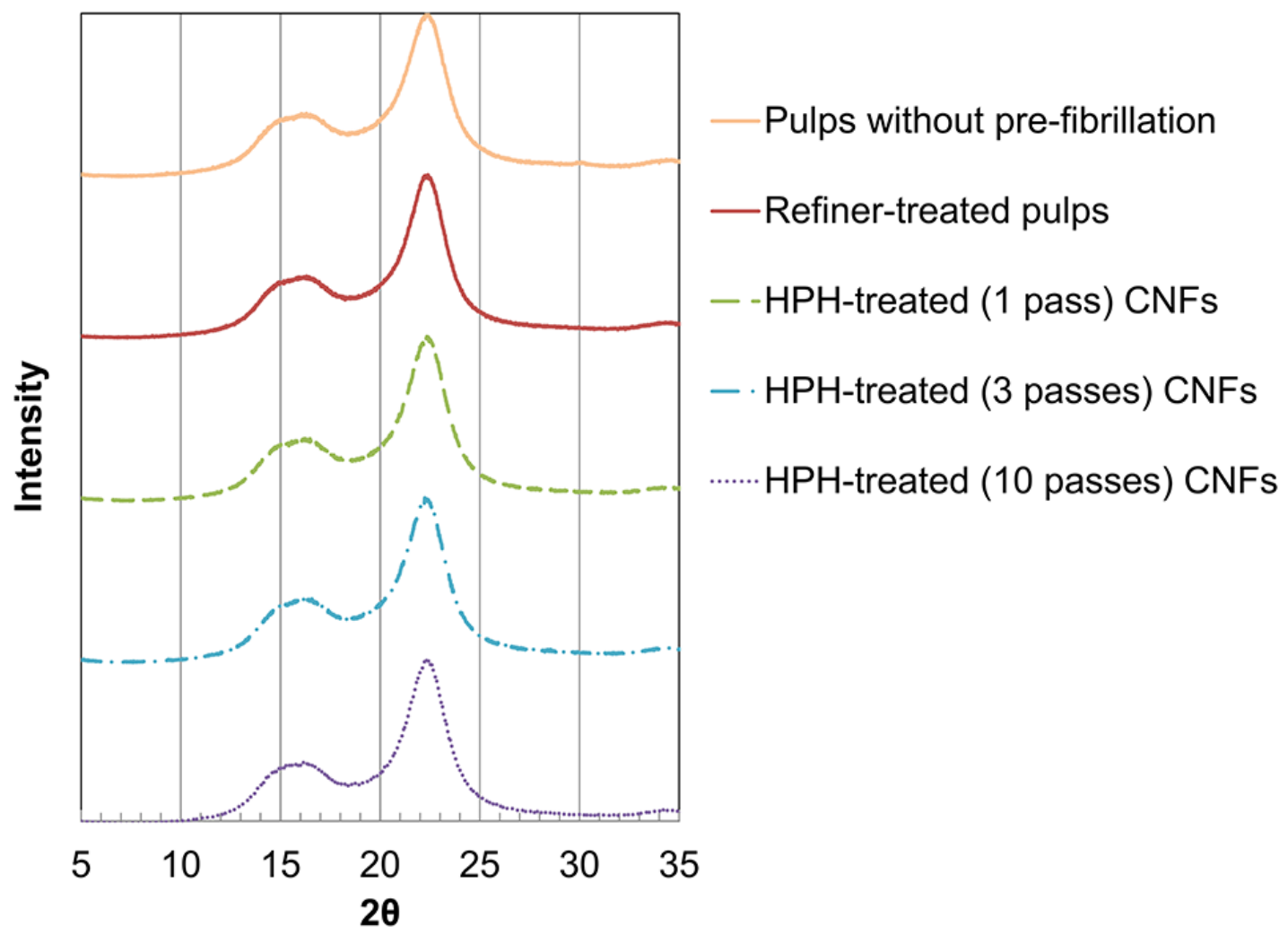
Figure 5

X-ray diffraction patterns of cellulose fibers.
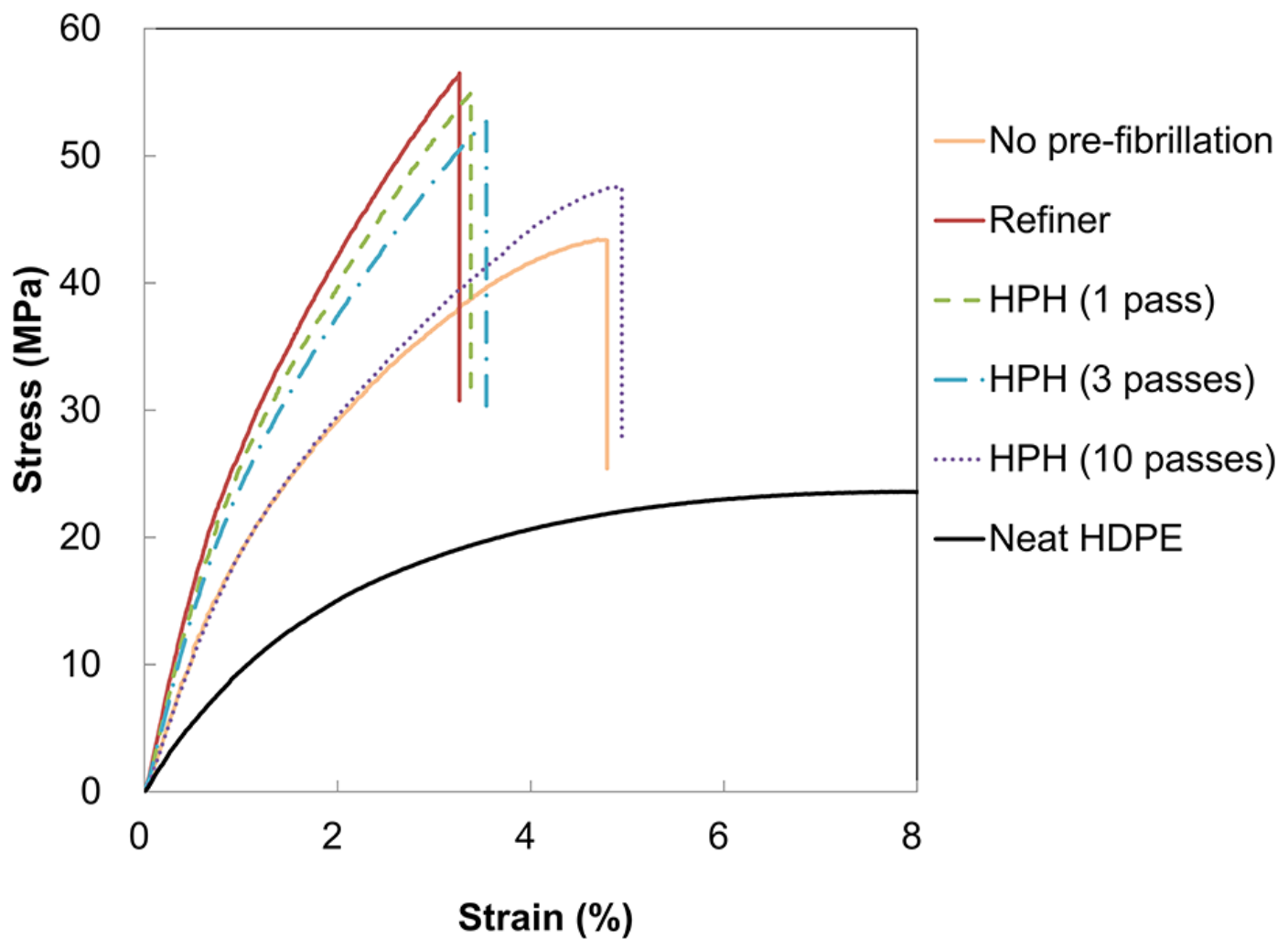
Figure 6

Typical stress−strain curves of composites from tensile tests.
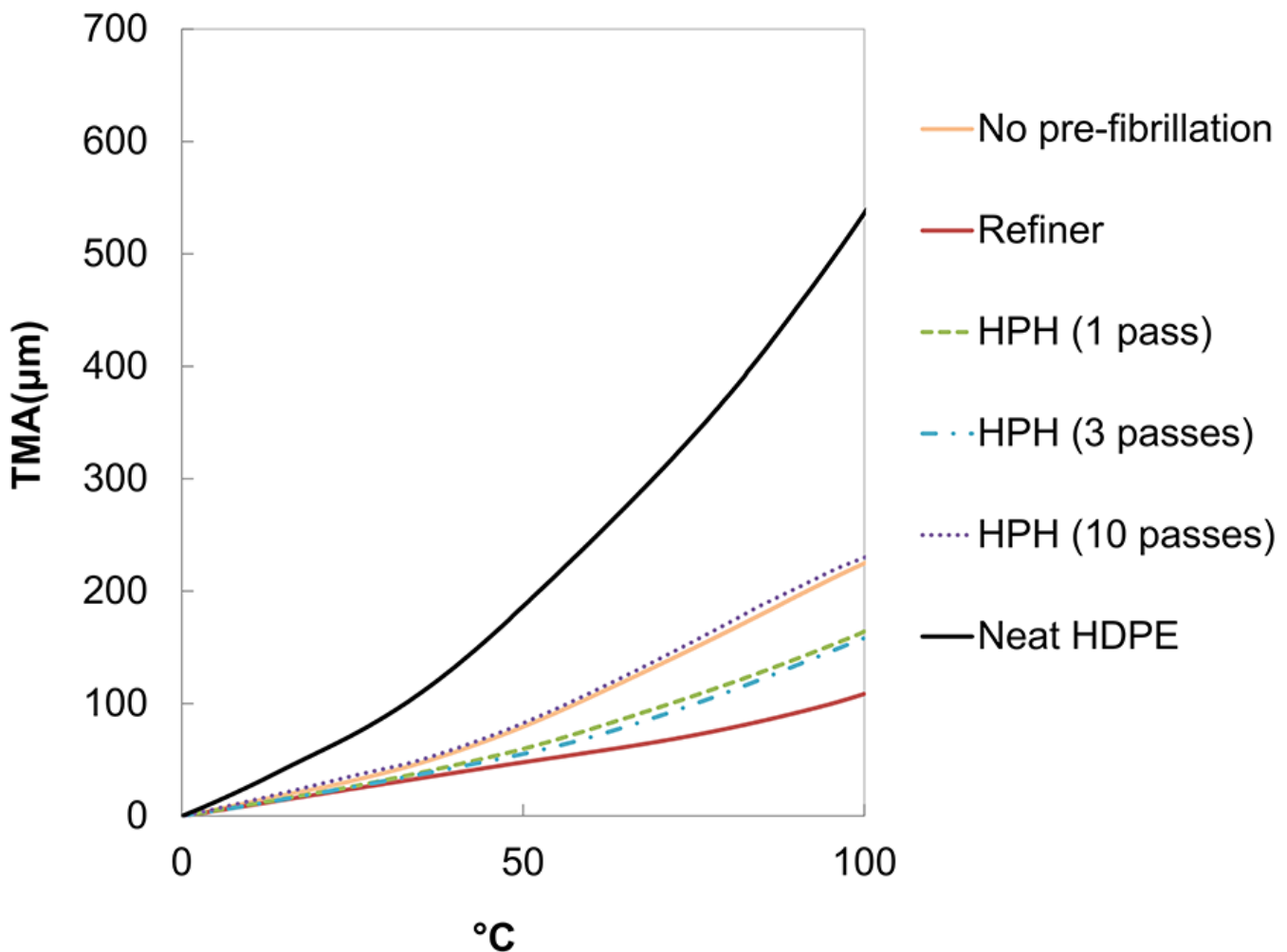
Figure 7

Elongation of composites versus temperature from thermomechanical tests.
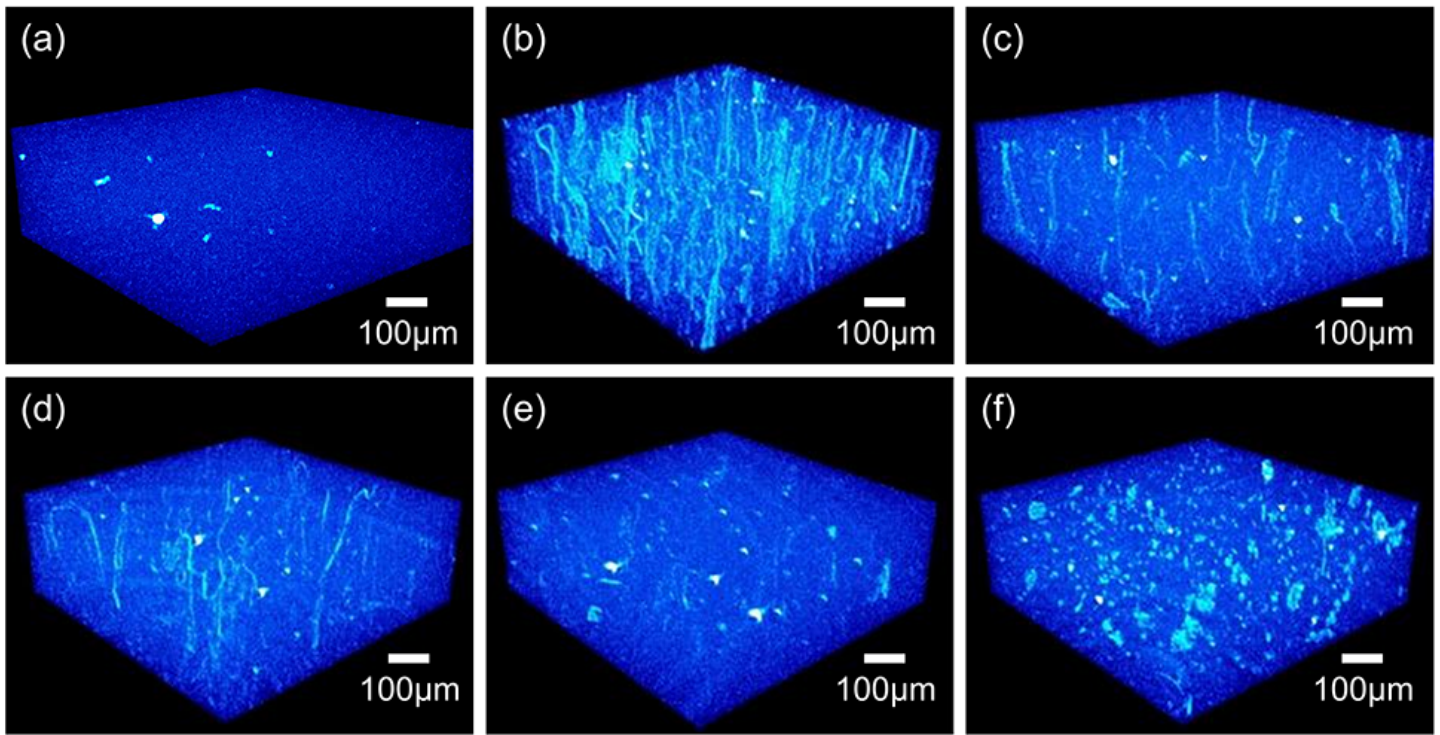
Figure 8

X-ray CT images of (a) neat HDPE and composites produced using: (b) pulps without pre-fibrillation, (c) refiner-treated pulps, (d) HPH-treated (1 pass) CNFs, (e) HPH-treated (3 passes) CNFs and (f) HPH-treated (10 passes) CNFs.
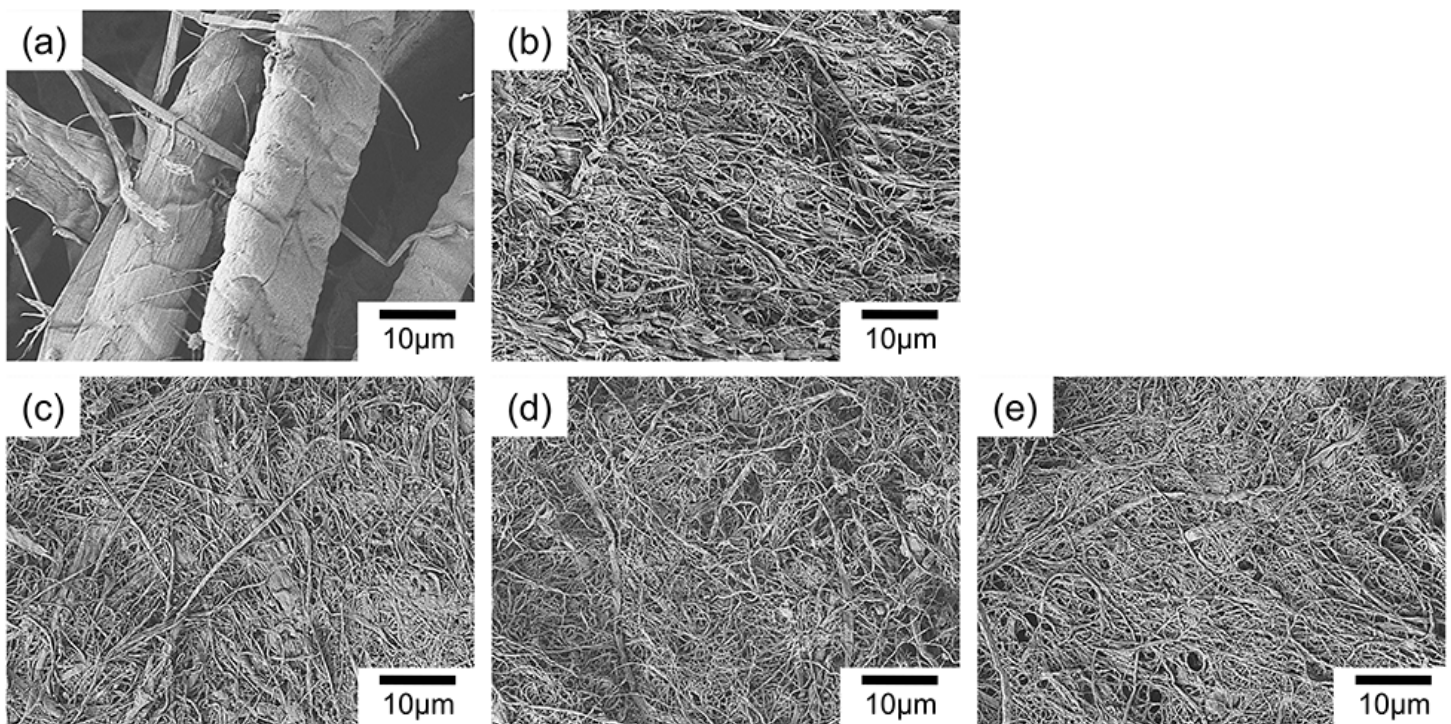

Figure 9

FE-SEM images of ASA-treated cellulose fibers in composites produced using: (a) pulps without pre-fibrillation, (b) refiner-treated pulps, (c) HPH-treated (1 pass) CNFs, (d) HPH-treated (3 passes) CNFs and (e) HPH-treated (10 passes) CNFs.

Figure 10

Length frequency distribution of ASA-treated cellulose fibers in composites produced using: (a) refiner-treated pulps, (b) HPH-treated (1 pass) CNFs, (c) HPH-treated (3 passes) CNFs and (d) HPH-treated (10 passes) CNFs.